

# A Novel Method to Evaluate Precision of Optical Implant Impressions with Commercial Scan Bodies—An Experimental Approach

Tabea Fluegge, DMD,<sup>1</sup> Wael Att, DMD,<sup>1,3</sup> Marc Metzger, MD, DDS,<sup>2</sup> & Katja Nelson, DDS<sup>1</sup>

<sup>1</sup>Department of Oral and Maxillofacial Surgery, University Medical Center, Freiburg, Germany

<sup>2</sup>Department of Oral Prosthodontics, University Medical Center, Freiburg, Germany

<sup>3</sup>Department of Restorative Dentistry Hamdan bin Mohammed College of Dental Medicine Mohammed bin Rashid University for Health and Medical Sciences, Dubai, UAE

## Keywords

Dental implants; dental implant-supported prosthesis; dental implant/abutment connection; laser scanning; CAD/CAM.

## Correspondence

Tabea Viktoria Fluegge, University Medical Center Freiburg, Department of Oral and Maxillofacial Surgery, Hugstetter Str. 55, 79106 Freiburg, Germany.  
E-mail: tabea.fluegge@uniklinik-freiburg.de.

*Presented at the 27th Annual Meeting of the German Association of Implantology, November 2013, Frankfurt, Germany*

*The authors deny any conflicts of interest.*

Accepted April 25, 2015

doi: 10.1111/jopr.12362

## Abstract

**Purpose:** Optical transfer is realized with system-specific transfer posts (scan bodies) mounted on dental implants or on implant analogs. This study presents a novel algorithm for creation of geometry on the surface of dental implant scan bodies and examines the precision of the optical acquisition of scan bodies and the precision of the position of the screw-tightened scan bodies on dental implant analogs.

**Materials and Methods:** Scan bodies of two different implant manufacturers (S1, S2), one with a horizontal and two with different conical implant-abutment geometries were screw tightened to implant analogs in stone casts with a 10 Ncm torque. The stone casts were scanned ten times with a dental lab scanner. Each scan body was removed and positioned ten times; after each repositioning, a scan was performed. The cylinder axis of every scan body and the occlusal horizontal scan body surface was virtually reconstructed. At the intersection of the cylinder axis and the horizontal plane a point was marked. The mean deviation of this point in consecutive scans and the angle between the scan body axes in the virtual models were measured, and the standard deviation was calculated. Statistical significance of the results was tested with a Kruskal-Wallis Test and Mann-Whitney U-test for pairwise comparison ( $p < 0.05$ ).

**Results:** The mean deviation of the angle between two scan bodies was 0.05° (SD 0.04°) (S1) and 0.14° (SD 0.08°) (S2). After detachment and repositioning of the scan bodies the mean deviation was 0.05° (SD 0.03°) (S1) and 0.16° (SD 0.08°) (S2). The mean deviation of the central point was 5.7 μm (SD 3.4 μm) without detachment and 4.9 μm (SD 2.6 μm) after detachment and repositioning (S1). For system S2 the mean deviation of the central point was 13.4 μm (SD 7.2 μm) after repeated scanning and 15 μm (SD 5 μm) after detachment, repositioning, and repeated scanning.

**Conclusions:** The precision of extraoral scanning of scan bodies is dependent on the scan body surface design and geometry. The precision of scanning with an extraoral model scanner differed between the scan body geometries and inter-scan body distances. The precision of dental implant scan body scanning was not significantly influenced by detachment and repositioning of the scan body.

For the CAD/CAM manufacturing of implant-supported restorations, the acquisition of a virtual model is required. This transfer of the intraoral situation to a virtual model is the first step of the digital workflow. The virtual model is either directly captured intraorally with an intraoral scanning device or extraorally through scanning of a dental cast with a dental lab scanner. In both cases transfer posts mounted on implants or on

implant analogs denoted as scan bodies are used to capture the correct implant position.<sup>1,2</sup>

The accuracy of the optical transfer is defined by its precision and trueness. The precision expresses how close repeated scans are to each other. The trueness describes how far the virtual model deviates from the actual dimensions of the object.<sup>3</sup>

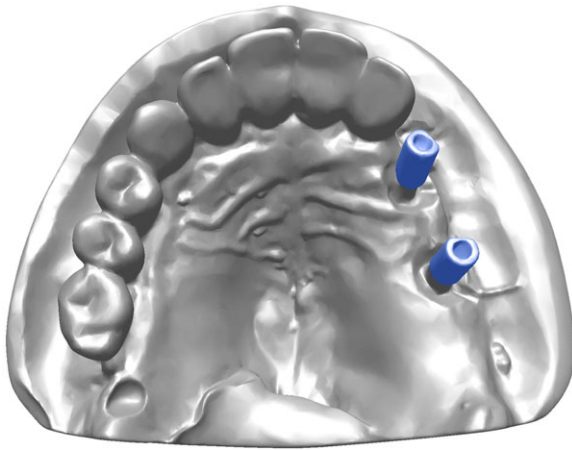


**Figure 1** Virtual model of stone casts with scan body S1R23 (maxillary left canine) and S2R25 (maxillary left second premolar) of system 1.

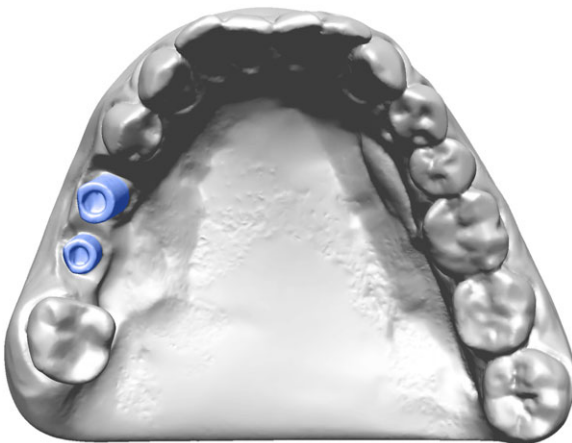


**Figure 2** Virtual model of stone cast and scan body S2R35 (mandibular left second premolar) and scan body S2R36 (mandibular left first molar) (S2).

The digital workflow based on intraoral scanning involves fewer clinical steps than extraoral digitization, which might show higher precision and efficiency for the CAD/CAM manufacturing of dental restorations.<sup>4</sup> On the other hand, intraoral conditions have been shown to compromise intraoral scan precision in areas with undercut (e.g., teeth) and in limited space between neighboring structures.<sup>5</sup>

Extraoral optical impressions of implants are indirectly captured with scan bodies positioned on implant analogs in a dental cast. A prerequisite to attain this dental cast is a conventional implant impression with suitable impression copings. Inaccuracies of the conventional impression and of the scanning process add to the overall error, which has been documented to vary between 15 and 67  $\mu\text{m}$  under experimental conditions.<sup>6-8</sup>

The geometry of scan bodies varies from a spherical design to a cylindrical design with diverse intermediate forms. The dimension relates to the respective system and to the implant diameter. The height of commercially available scan bodies ranges from 3 to 17 mm. The requirements of the surface ge-

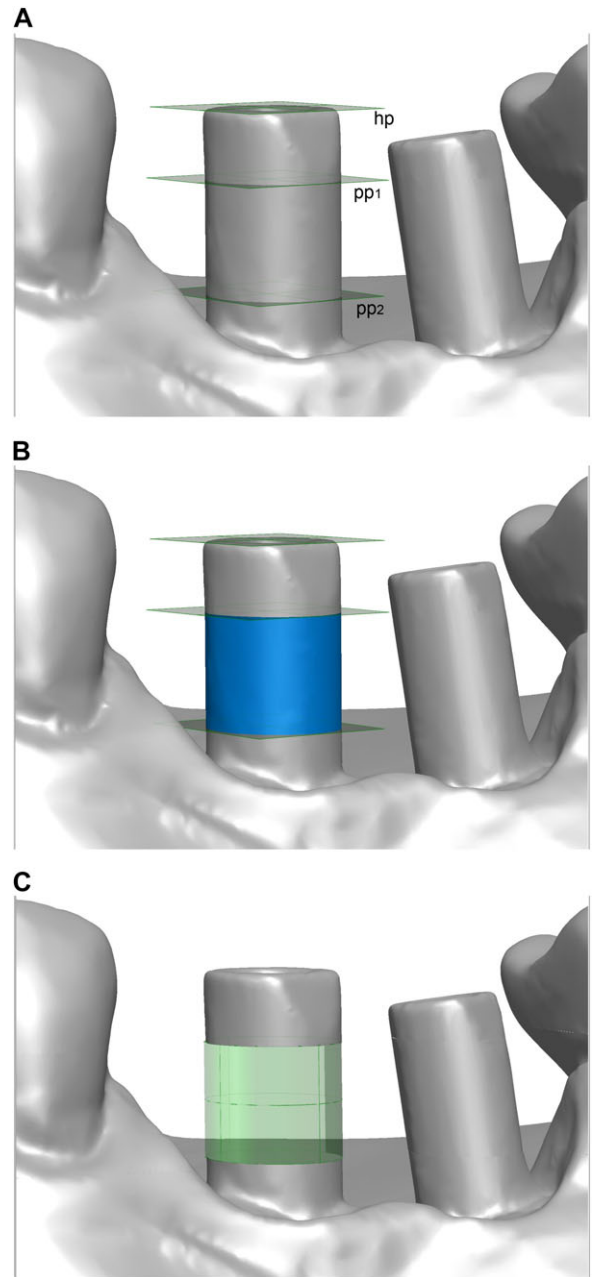


**Figure 3** A: Plane (yellow) on horizontal surface of scan body and two parallel planes with a defined distance of 3 and 4 mm respectively; B: Marked surface (blue) between parallel planes for the creation of a cylinder; C: Cylinder derived from scan body surface.

ometry and dimension of the implant scan body for an accurate transfer of the implant position to the virtual model have not been analyzed. The literature does not provide information on the precision of capturing the dimensions of the scan bodies in regard to different surface geometries and dimensions, different designs of the implant/abutment interface, and on deviations caused by repositioning of scan bodies in the implant or implant analog.

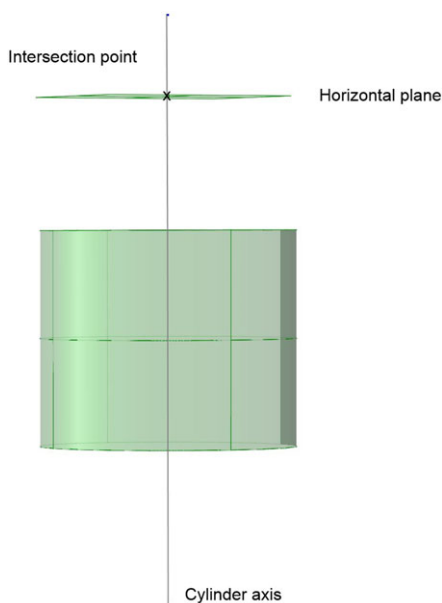


**Figure 4** Central vector derived from cylinder, horizontal plane and intersection point between horizontal plane and central vector of the cylinder.

This experimental study presents an algorithm to create a geometric model on the basis of a surface scan of commercially available implant scan bodies. The precision of capturing the scan body geometry was tested using two scan body designs with different sizing. Additionally, the precision of dental implant scan body digitization with a dental lab scanner (D250) and the position stability of dental implant scan bodies with different implant/abutment connection geometries were compared using repeated scans.

## Materials and methods

### Stone cast production and scanning

Dental casts of two different partially edentulous patients each with two implant analogs of different implant systems and the corresponding scan bodies were used (Figs 1 and 2). One stone cast of each patient was produced with Type IV stone (U180; Picodent, Wipperfürth, Germany) based on polyether impressions (Impregum Penta; 3M ESPE, Seefeld, Germany) with open-tray impression posts from the corresponding system using a splinted pick-up technique and an individual impression tray.<sup>6,8-10</sup> The impressions were immersed in a disinfecting solution for 10 minutes and poured 4 hours after impression taking. Within 24 to 48 hours after production, the dental casts were digitized with each scanning system.

The maxillary stone cast of one patient had two implant analogs of system 1 (S1) (Camlog Biotechnologies, Basel, Switzerland) located in the left canine and second premolar region without teeth posterior of the implants. The implant/abutment interface has a butt-joint geometry: canine left (S1R23; REF J3010.3800) and second premolar left (S1R25; REF J3010.430). The mandibular stone of the other patient had implant analogs of system 2 (S2) (Straumann, Basel,

Switzerland) in the regions of the left second premolar and the left first molar each with a different conical implant/abutment connection (second premolar left: S2R35; Tissue Level REF 048.124 and first molar left: S2R36; Bone Level REF 025.4101). To comply with the manufacturer's protocol to tighten the screws manually, a torque of 10 Ncm was applied with the system-specific ratchet. This was recommended by Gross *et al* as being equivalent to manual screw tightening.<sup>11</sup>

Scan bodies S1R23 (REF K2600.3810) and S1R25 (REF K2600.4310) were mounted on the implant analogs with a screwdriver (REF J5316.0502) and a torque ratchet (REF J5320.1030) set to 10 Ncm. The scan bodies had a height of 10 mm and a diameter of 4.3 mm. The corresponding scan bodies in the mandibular model were mounted with a screwdriver (REF 046.402) and a torque ratchet (REF 046.119/046049). The torque ratchet was calibrated prior to use in this study. In the region of the second premolar on the left, the corresponding scan body (S2R35) had a height of 10 mm and a diameter of 5 mm (REF 048.168), and in the region of the first molar the corresponding scan body (S2R36) was 9 mm high and 4 mm in diameter (REF 025.4915).

The following experimental protocol was performed:

1. Each stone cast with the positioned scan bodies was scanned ten times with a laser scanner (D250; 3Shape, Copenhagen, Denmark) without detachment of the model from the scanning tray between the scanning cycles.
2. The scan bodies were detached from the stone cast and repositioned. After positioning and tightening with the same torque (10 Ncm), scanning of the stone cast was repeated. The procedure of detachment and positioning was repeated nine times, and a scan was obtained after every positioning.

### Data handling

Virtual models were derived from scanning in an STL-format (Stereolithography; 3D Systems, Rock Hill, SC) and imported in Rapidform XOR<sub>2</sub> software (INUS Technologies, Seoul, South Korea). Surfaces were created on the basis of the imported models. The surfaces of the consecutive models were placed in the same coordinate system. With the implemented best-fit algorithms searching for the shortest distance of corresponding points of two surfaces, the models were registered.<sup>12</sup> The applied mean-square-distance-metric ensured a median alignment of the virtual models.<sup>13</sup> The first model served as reference, and the following nine models were each registered onto the first models. The surface of the scan bodies was blinded during the registration process to guarantee that only the unchanged structures (teeth and gingiva) were used for registration.

### Algorithm for a geometric model of the surface of scan bodies

From the cylindrical surfaces of the scan bodies the cylinder axes were derived to measure canting deviations,<sup>14</sup> and the central point on the horizontal surface of the cylinder was used to measure spatial deviations. With manual determination of surface points on the upper horizontal surface of the scan body

a horizontal plane (hp) was created. Two parallel planes to the hp were created with a distance of 4 mm (S1R23, S1R25, and S2R35) and 3 mm (S2R36). With these planes the middle segment of each scan body was cut out, and its surface information was used to create a cylinder with a least-square fitting algorithm (Fig 3).<sup>15</sup> The central vector (v) along the cylinder axis was calculated with the software. A point (p) at the intersection of the horizontal plane and the cylinder axis (ca) was marked (Fig 4). The intersection point (p) and the cylinder axis (ca) were derived from each scan body and were used for the determination of its position.

**Precision of geometric models of dental implant scan bodies**

The precision of the algorithm was determined with five repeated measurements of one scan body in the virtual model derived from the first scan of S1R23, S1R25, S2R35, and S2R36. The cylinder axis (ca) and the intersection point (p) were marked five times as described above. The Euclidean distances between the intersection points and the angle between the cylinder axes were measured. The mean distance and angle and the standard deviation were calculated.

**Precision of scanning dental implant scan bodies**

To determine the precision of the scanning process of dental implant scan bodies, ten consecutive scans without manipulation of the model were acquired. The virtual models were registered and measured with the algorithm described above. The mean distance of the intersection points (p) and angle between the cylinder axes (ca) and their standard deviation were recorded.

**Precision of dental implant scan body position in implant analogs**

The precision of the implant scan body position was evaluated with virtual models derived from ten consecutive scans after detachment and repositioning of the scan bodies. The distance between the intersection points and the angle between the cylinders' axes were measured after registration of the virtual models as described above.

**Statistical evaluation**

Spatial deviations and angular deviations of each scan body were compared between S1 and S2 using a Mann-Whitney test for pairwise comparison. The precision of geometric model creation, scanning, and the scan body position were compared with a Kruskal-Wallis test and with a Mann-Whitney U-test for pairwise comparison. The relation between each measurement and the system (S1 and S2) was evaluated with a nonparametric test as in Brunner et al.<sup>16</sup> The level of significance was set to  $p < 0.05$ . Statistical analysis was conducted with SPSS 22 (SPSS Inc., Chicago, IL).

**Table 1** Mean distances and standard deviations (SD) of the intersection point (p) in  $\mu\text{m}$  and mean angles of the repeated measurements of the same virtual model to evaluate the repeatability of the algorithm

	Mean distance in $\mu\text{m}$ (SD)	Mean angle in degrees (SD)
S1R23	2 (1)	0.04 (0.03)
S1R25	3.3 (3)	0.05 (0.04)
S2R35	2 (1)	0.03 (0.01)
S2R36	5.6 (3)	0.07 (0.03)

**Table 2** Mean distances and standard deviations (SD) of the intersection point (p) in  $\mu\text{m}$  and mean angles of the measurements of virtual models produced from consecutive scans to evaluate the precision of the scanning method

	Mean distance in $\mu\text{m}$ (SD)	Mean angle in degrees (SD)
S1R23	6.2 (2.9)	0.03 (0.01)
S1R25	5.3 (3.9)	0.06 (0.05)
S2R35	12.6 (3.1)	0.12 (0.05)
S2R36	14.1 (10)	0.16 (0.09)

**Results**

**Precision of the geometric model**

The precision of the presented algorithm was determined with five repeated measurements of each scan body in one scan. For S1 the deviation was on average 2  $\mu\text{m}$  (S1R23) and 3.3  $\mu\text{m}$  (S1R25) for the intersection point (p), 0.044° (S1R23) and 0.045° (S1R25), respectively, for the cylinder axes. For S2 the deviation averaged 2  $\mu\text{m}$  (S2R35) and 5.6  $\mu\text{m}$  (S2R36) for p, and 0.031° (S2R35) and 0.066° (S2R36) for the cylinder axes (Table 1).

**Precision of scanning and position of dental implant scan bodies**

After repeated scanning, the mean distance of deviation of the intersection point (p) was 5.7  $\mu\text{m}$  (SD 3.4  $\mu\text{m}$ ) for S1. Both scan bodies showed similar values: mean for S1R23: 6.2  $\mu\text{m}$  (SD 2.9  $\mu\text{m}$ ) and mean for S1R25: 5.3  $\mu\text{m}$  (SD 3.9  $\mu\text{m}$ ). The mean deviation of the intersection point (p) after detachment and positioning of the scan body was 4.9  $\mu\text{m}$  (SD 2.6  $\mu\text{m}$ ) for S1. S1R23 had a mean deviation of 3.2  $\mu\text{m}$  (SD 1.2  $\mu\text{m}$ ), and S1R25 had a significantly different mean deviation of 6.7  $\mu\text{m}$  (SD 2.3  $\mu\text{m}$ ). The mean distance for the intersection point (p) after repeated scanning was 13.4  $\mu\text{m}$  (SD 7.2  $\mu\text{m}$ ) for S2, and the two scan bodies each had the following values: S2R35: mean 12.6  $\mu\text{m}$ , SD 3.1  $\mu\text{m}$ ; S2R36: mean 14.1  $\mu\text{m}$ , SD 10  $\mu\text{m}$ . After detachment and repositioning the mean deviance of the intersection point (p) in S2 was 14.9  $\mu\text{m}$  (SD 5.0  $\mu\text{m}$ ). The mean distances of the two different scan bodies were 16.3  $\mu\text{m}$  (SD 4.4  $\mu\text{m}$ ) for S2R35 and 13.4  $\mu\text{m}$  (SD 5.3  $\mu\text{m}$ ) for S2R36. The distance and angulation values for each scan body are displayed in Table 2 and Table 3.

**Table 3** Mean distances and standard deviations (SD) of the intersection point ( $p$ ) in  $\mu\text{m}$  and mean angles of the measurements of virtual models produced from scans after detachment and repositioning of the scan bodies to evaluate the precision of the dental implant scan body position

	Mean distance in $\mu\text{m}$ (SD)	Mean angle in degrees (SD)
S1R23	3.2 (1.2)	0.04 (0.02)
S1R25	6.7 (2.3)	0.07 (0.04)
S2R35	16.3 (4.4)	0.155 (0.04)
S2R36	13.4 (5.3)	0.16 (0.1)

For S1, the mean deviation of the vector between the consecutive scans was  $0.05^\circ$  (SD  $0.04^\circ$ ). After detachment and positioning the deviation was not significantly different (mean  $0.05^\circ$  and SD  $0.03^\circ$ ).

The mean deviation of the cylinder axes without detachment of the scan bodies of S2 was  $0.14^\circ$  (SD  $0.08^\circ$ ). With detachment and repositioning of the scan bodies the mean deviation of the cylinder axes was  $0.16^\circ$  (SD  $0.08^\circ$ ).

The precision of the geometric model, of scanning, and of scan body position were significantly different for the distance ( $p < 0.001$ ) and the angle ( $p = 0.01$ ). Pairwise comparison demonstrated significant differences between the precision of the geometric model and precision of scanning (distance:  $p < 0.001$ ; angle:  $p = 0.02$ ), the precision of geometric model and the precision of scan body position (distance:  $p < 0.001$ ; angle:  $p < 0.004$ ), but no significant difference between the precision of scanning and the precision of scan body position (distance:  $p = 0.84$ ; angle:  $p = 0.46$ ).

The angular and spatial deviations of the scan bodies were significantly different between S1 and S2 ( $p < 0.001$ ). For S1, precision of the geometric model, precision of scanning, and precision of scan body position were significantly different regarding the distance ( $p = 0.02$ ) but not significantly different regarding the angle between two scan bodies ( $p = 0.65$ ). For S2, repeated geometric model creation, scanning, and repositioning caused significant differences regarding the distance ( $p < 0.001$ ) and the angle ( $p = 0.001$ ); however, when comparing S1 with S2, measured deviations were significantly lower for S1, which was evident without detachment ( $p < 0.05$ ) as well as with detachment and repositioning ( $p < 0.05$ ). The analysis after Brunner demonstrated a significant interdependent influence of the system and the measurement (geometric model creation, scanning and scan body position) related to the distance ( $p = 0.004$ ) and the angle ( $p = 0.002$ ). The angular and spatial deviations of the scan bodies of S1 and S2 are displayed in Figures 5 and 6, respectively

## Discussion

The precision of three different aspects of the optical transfer of dental implants was studied: (a) the precision of the geometric model of the surface of dental implant scan bodies; (b) the precision of scanning implant scan bodies, and (c) the precision of the scan body position in dental implant analogs. Precision is defined as one of two aspects that constitute the term of accuracy. Precision describes how close repeated measurements

are to each other. The second aspect of accuracy is trueness and describes how far a measurement deviates from the actual object.<sup>3</sup> Therefore, the accurate transfer of dental implant positions relies on the precision and trueness of the method. To detect the trueness of virtual dental models a reproduction of the actual intraoral situation has to be produced. This fact implies that the trueness may only be approximated by minimizing possible errors of a transfer system.<sup>17-21</sup> This study focused on the precision as a constituent factor for an accurate optical transfer of different implant scan bodies.

The registration and evaluation of surface scans using best-fit algorithms without the extraction of surface characteristics<sup>9,10</sup> or with the additional definition of surface characteristics of experimental transfer bodies<sup>14,22</sup> and scan bodies<sup>2</sup> was documented in different studies. The creation of common characteristics on 3D surfaces to compare different commercially available scan bodies has not been conducted before. This study presents a novel method to capture the geometry of the surface of dental implant scan bodies to determine their position and orientation in a coordinate system.

For the creation of geometries on the basis of the cylindrical scan bodies only the points defining the horizontal plane were manually chosen. Further identification of surface characteristics was conducted with a least-square fitting algorithm implemented in the software.<sup>15</sup> The precision of the geometric model (between 2 and  $5.6 \mu\text{m}$ ) for the tested scan bodies S1R23, S1R25, S2R35, and S2R36 showed a tendency to lower precision for a shorter and narrower scan body (S2R36), implying that the surface characteristics of the commercially available scan bodies in this study are suitable to create a geometric form and record their orientation and position within the dental arch.

Comparable to the procedure in this study, optical digitization of implants to manufacture implant-supported prosthetics involves scan bodies with standardized geometric dimensions. In the current CAD/CAM workflow the acquired image of the scan body is superimposed with the stored data of the corresponding CAD model of the scan body. This procedure allows the calculation of the actual implant position and compensates for minor scanning artifacts. Registration of two surfaces is accomplished with an iterative closest point algorithm. Every surface vertex in a point cloud is matched with the nearest vertex in the neighboring point cloud using a mean-square-distance metric to ensure a median alignment and elimination of outliers.<sup>13</sup> However, the more artifacts present in a scan, the less accurate a geometrical shape can be matched or created on the information of the scan body surface.

The precision of angular and spatial measurements was significantly different between S1 and S2. The scanning of implant scan bodies of S2 demonstrated higher variations than S1 both regarding the spatial and angular deviations. Multiple reasons including the error caused by repeated scanning of one stone cast, the registration error, and the proximity of neighboring structures could be discussed in this context. The stone cast with scan bodies of S1 was partially edentulous in the posterior dental arch, and the scan bodies were placed in the region of the canine and the second premolar. In comparison, the stone cast containing scan bodies of S2 had a smaller inter-scan body distance (second premolar and first molar) and scan body/tooth distance. Scan bodies were positioned closer to each other and

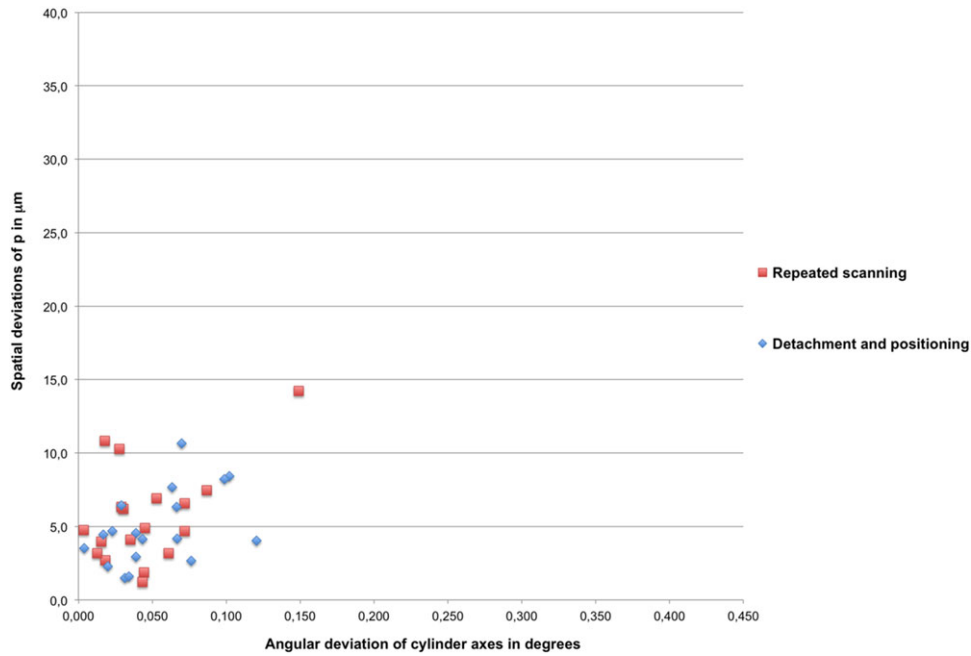


**Figure 5** Spatial and angular deviations of each scan body in every consecutive scan without detachment (red rectangles) and after detachment and positioning (blue rectangles) in S1 (S1R23 and S1R25).

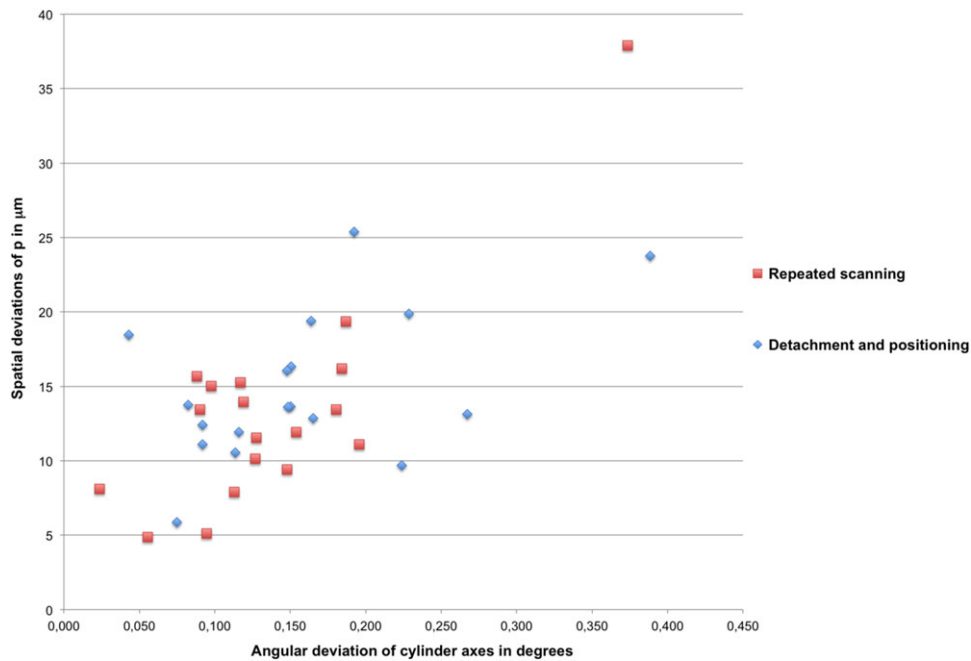


**Figure 6** Spatial and angular deviations of each scan body in every consecutive scan without detachment (red rectangles) and after detachment and positioning (blue rectangles) in S2 (S2R35 and S2R36).

to the neighboring second molar. The less precise digital capturing of the geometry of the scan bodies of S2 might be a result of the limited space and therefore compromised scanning conditions. Future studies should evaluate the influence of the distance between implant scan bodies, including single-tooth

spaces and cross-arch distances to elucidate the correlation of a registration error and spacing.

The precision of scanning full-arch stone casts with the dental lab scanner was stated as  $10 \mu\text{m}$ <sup>5,23</sup> and  $5 \mu\text{m}$ .<sup>2</sup> Previous studies investigated the accuracy of digital implant impressions

with optical acquisition methods and different experimental transfer bodies. Del Corso *et al* measured the accuracy of scanning markers on implant analogs with a laser scanner and a coordinate measuring machine (CMM) with known accuracy of  $0.04 \mu\text{m}$ . The measured deviations were between  $14$  and  $21 \mu\text{m}$  for the laser scanner with reference to the CMM.<sup>20</sup> The laser scanner with a fringe light pattern was comparable to the device used in this study; however, the size and geometry of the scan bodies were not disclosed. They were assembled using a steel base and a ceramic body and were scanned with CMM first using a non-specified software-supported data interpretation. The identification of reference points on their surface was not described. Ortorp *et al* compared the acquisition of implant positions with photogrammetry and conventional impressions *in vitro*. For the creation of virtual models, scan bodies of unknown dimensions were placed in the implant analogs of each model and were acquired with a CMM. The virtual models were registered and points on the surface of the scan bodies were measured. Neither the error of registration nor the determination of surface points was described. Deviations of the implant position from the master cast were between  $24 \mu\text{m}$  (photogrammetry) and  $25 \mu\text{m}$  (polyether).<sup>24</sup>

Holst *et al* assessed the precision of a dental touch-probe scanner ( $9 \mu\text{m}$ ) and an optical scanner ( $11 \mu\text{m}$ ) and compared it to the precision of a CMM ( $0 \mu\text{m}$ ).<sup>19</sup> The optical and touch-probe scanners use a different protocol than the laser scanner used in this study. The dimensions of the transfer posts (implant position locators) and the algorithm to find their center point used for measurements was not described. The results of this study for the scanning precision were comparable to the results of this study regarding S2 ( $13.4 \mu\text{m}$ ). With S1 ( $5.7 \mu\text{m}$ ) the precision was higher than in the above-mentioned studies.

Stimmelmayer *et al* studied the precision of the scan body position in implant analogs and found a mean deviation of defined points in ten consecutive scans of  $11 \mu\text{m}$ .<sup>2</sup> The same implant system was used in this study (S1), and deviations between the central cylinder points were on average  $5.7 \mu\text{m}$ . Stimmelmayer *et al* did not display the deviations related to spatial coordinates ( $x$ ,  $y$ , and  $z$ ) and did not display angular deviations.<sup>2</sup> The scan bodies were cut with a reference plane after registration, and multiple points on that plane were used for measurement.

With regard to the presented studies the sensitivity of optical acquisition must be discussed. The deviations for repeated scanning are considered to result from the error of scanning, registration, and measurement. The precision of a CMM and dedicated sample bodies remains superior to the optical scanning device used in this study.<sup>17-21</sup> The results derived with a dental lab reference scanner presented in this study might be compared to data derived from intraoral scanning of dental implant scan bodies to further study the influence of scanning conditions on its accuracy.

The precision after detachment and repositioning of implant scan bodies was not significantly different compared to repeat scanning without detachment. The scan bodies of S2 were placed on implants with a different design of their conical implant-abutment connection (S2R35:  $8^\circ$  cone angle, S2R36:  $15^\circ$  cone angle); however, the difference in the cone angle of the conical connection geometry did not seem to influence the

position of the optical scan body. The same observation was made after detachment and repositioning of the S1 scan bodies. No significant changes of the scan body position were recorded; therefore, the precision of the scan body acquisition might not depend on the geometry of the connection. All scan bodies were made of the same material (PEEK) and mounted on stone casts produced from conventional impressions each of an original clinical situation. The trueness of the transfer of the intraoral situation to the model is not considered within this study.<sup>9,24</sup> The spatial and angular deviations assessed in this study do not express rotational movements of the scan bodies in the implant analogs. No conclusion can be drawn regarding the rotational freedom of the abutment geometries. Semper *et al*<sup>18</sup> measured the position stability of various implant/abutment connections (IAC) and the rotational, canting, and vertical changes of the position of the abutment after detachment and repositioning. The canting deviations were between  $0.0^\circ$  and  $0.31^\circ$  and were not significantly different between the systems. The canting deviations in our study were lower for the butt-joint connection ( $0.05^\circ$  after repeated scanning and after detachment and repositioning) and for the conical connections ( $0.14^\circ$  after repeated scanning and  $0.16^\circ$  after detachment and repositioning). The vertical changes in the compared study by Semper *et al* ranged from  $4$  to  $5 \mu\text{m}$  for butt-joint connections and  $26$  to  $29 \mu\text{m}$  for conical connections. The deviation of the scan bodies placed in the conical IAC in our study ( $13.4 \mu\text{m}$  after repeated scanning and  $14.9 \mu\text{m}$  after detachment and repositioning) was lower, while all the butt-joint connections in this study had a comparable spatial deviation ( $5.7 \mu\text{m}$  after repeated scanning and  $4.9 \mu\text{m}$  after detachment and repositioning).<sup>18</sup> The different material of the scan bodies (PEEK) compared to conventional abutments (titanium), along with a difference in the torque applied, might be a reason for the different results.

It is known that there is a deviation in abutment position after repositioning of the abutment, and this variation depends on the geometry of the IAC.<sup>18,25</sup> Multiple positioning of the scan bodies did not show a significant variation in the position stability compared to multiple scanning. The trueness of the transfer of the position from the scan body to the definitive abutment is not verified with the present data.

## Conclusions

The presented algorithm is an adequate tool to extract surface information of commercially available scan bodies. The precision of scanning with an extraoral model scanner differed between the scan body geometries and inter-scan body distances. The precision of dental implant scan body scanning was not significantly influenced by detachment and repositioning of the scan body.

## References

1. Joda T, Wittneben JG, Bragger U: Digital implant impressions with the "Individualized Scanbody Technique" for emergence profile support. *Clin Oral Implants Res* 2014;25:395-397
2. Stimmelmayer M, Guth JF, Erdelt K, *et al*: Digital evaluation of the reproducibility of implant scanbody fit-in *in vitro* study. *Clin Oral Investig* 2012;16:851-856

3. ISO-5725-1. Accuracy (trueness and precision) of measurement methods and results—Part 1: general principles and definitions. Geneva, International Organization for Standardization, 1994, p. 17
4. Beuer F, Schweiger J, Edelhoff D: Digital dentistry: an overview of recent developments for CAD/CAM generated restorations. *Br Dent J* 2008;204:505-511
5. Fluegge TV, Schlager S, Nelson K, et al: Precision of intraoral digital dental impressions with iTero and extraoral digitization with the iTero and a model scanner. *Am J Orthod Dentofacial Orthop* 2013;144:471-478
6. Vigolo P, Majzoub Z, Cordioli G: Evaluation of the accuracy of three techniques used for multiple implant abutment impressions. *J Prosthet Dent* 2003;89:186-192
7. Hsu CC, Millstein PL, Stein RS: A comparative analysis of the accuracy of implant transfer techniques. *J Prosthet Dent* 1993;69:588-593
8. Kim S, Nicholls JJ, Han CH, et al: Displacement of implant components from impressions to definitive casts. *Int J Oral Maxillofac Implants* 2006;21:747-755
9. Stimmelmayer M, Erdelt K, Guth JF, et al: Evaluation of impression accuracy for a four-implant mandibular model—a digital approach. *Clin Oral Investig* 2012;16:1137-1142
10. Stimmelmayer M, Guth JF, Erdelt K, et al: Clinical study evaluating the discrepancy of two different impression techniques of four implants in an edentulous jaw. *Clin Oral Investig* 2013;17:1929-1935
11. Gross M, Kozak D, Laufer BZ, et al: Manual closing torque in five implant abutment systems: an in vitro comparative study. *J Prosthet Dent* 1999;81:574-578
12. Zhu L, Barhak J, Srivatsan V, et al: Efficient registration for precision inspection of free-form surfaces. *Int J Adv Manufacturing Technol* 2007;32:505-515
13. Besl PJ, McKay ND. Method for registration of 3-D shapes. *IEEE Trans Pattern Anal Mach Intel* 1992;14:239-256
14. vander Meer WJ, Andriessen FS, Wismeijer D, et al: Application of intra-oral dental scanners in the digital workflow of implantology. *PloS One* 2012;7:e43312
15. Pratt V: Direct least-squares fitting of algebraic surfaces. *SIGGRAPH Comput Graph* 1987;21:145-152
16. Brunner E, Domhof S, Langer F: *Nonparametric Analysis of Longitudinal Data in Factorial Experiments*. New York, Wiley, 2002
17. Karl M, Graef F, Schubinski P, et al: Effect of intraoral scanning on the passivity of fit of implant-supported fixed dental prostheses. *Quintessence Int* 2012;43:555-562
18. Semper W, Heberer S, Mehrhof J, et al: Effects of repeated manual disassembly and reassembly on the positional stability of various implant-abutment complexes: an experimental study. *Int J Oral Maxillofac Implants* 2010;25:86-94
19. Holst S, Persson A, Wichmann M, et al: Digitizing implant position locators on master casts: comparison of a noncontact scanner and a contact-probe scanner. *Int J Oral Maxillofac Implants* 2012;27:29-35
20. Del Corso M, Abà G, Vazquez L, et al: Optical three-dimensional scanning acquisition of the position of osseointegrated implants: an in vitro study to determine method accuracy and operational feasibility. *Clin Implant Dent Relat Res* 2009;11:214-221
21. Wegner K, Weskott K, Rehmann P, et al: TAGUNGSBEITRAG-Untersuchung beeinflussender Faktoren auf die Übertragungsgenauigkeit von Implantatabformungen. *Deutsche Zahnärztliche Zeitschrift* 2011;66:754
22. Del Corso M, Aba G, Vazquez L, et al: Optical three-dimensional scanning acquisition of the position of osseointegrated implants: an in vitro study to determine method accuracy and operational feasibility. *Clin Implant Dent Relat Res* 2009;11:214-221
23. Persson A, Andersson M, Oden A, et al: A three-dimensional evaluation of a laser scanner and a touch-probe scanner. *J Prosthet Dent* 2006;95:194-200
24. Ortorp A, Jemt T, Back T: Photogrammetry and conventional impressions for recording implant positions: a comparative laboratory study. *Clin Implant Dent Relat Res* 2005;7:43-50
25. Semper W, Kraft S, Mehrhof J, et al: Impact of abutment rotation and angulation on marginal fit: theoretical considerations. *Int J Oral Maxillofac Implants*. 2010;25:752-758



Copyright of Journal of Prosthodontics is the property of Wiley-Blackwell and its content may not be copied or emailed to multiple sites or posted to a listserv without the copyright holder's express written permission. However, users may print, download, or email articles for individual use.